Liquid–Vapor Equilibria of Linear Kihara Molecules

Carlos Vega,* Santiago Lago,

Departamento de Quimica Fisica, Facultad de Ciencias Quimicas, Universidad Complutense, 28040 Madrid, Spain

Enrique de Miguel, and Luis F. Rull

Departamento de Fisica Atomica Molecular y Nuclear, Universidad de Sevilla, Aptdo 1065, Sevilla 41080, Spain *(Received: March 12, 1992; In Final Form: May 14, 1992)*

The liquid–vapor equilibria of the linear Kihara fluid with elongations $L^* = L/\sigma = 0.3$, 0.6, and 0.8 is studied. We compare the prediction of a recently proposed perturbation theory of Kihara fluids with the Monte Carlo results obtained by using the Gibbs ensemble simulation technique. The agreement between the theoretical predictions and the simulation results was found to be very good from the triple point up to 0.9 times the critical temperature. The molecular anisotropy increases the slope of the vapor pressure curve and provokes deviations from the principle of corresponding states. The deviations from the principle of corresponding states with molecular elongation found for linear Kihara fluids are similar to those found in previous studies for the two-center Lennard-Jones model.

I. Introduction

The statistical mechanics of nonspherical molecules have received much attention during the past decade.[1,2] Integral equations[3-6] and perturbation theories[7-13] have now been developed for several nonspherical models. The nonspherical interaction has been typically described by using three different kinds of potential models, namely the site–site model,[1] the Kihara model,[14] and the Gaussian overlap model.[15] Although these potentials models differs each other in the details, it is expected that any among them could be used to illustrate the effect of molecular anisotropy on thermodynamical properties. In particular, the effects of molecular shape on vapor–liquid equilibria and on deviations from the principle of corresponding states stand as very interesting problems. Understanding the effect of molecular shape on phase equilibria should be considered as a first goal. Later studies, including both molecular anisotropy and multipolar forces, should benefit from this knowledge. In this context, two theoretical studies of the vapor–liquid equilibria of two center Lennard-Jones (2CLJ) molecules have recently appeared.[16,17] Fischer et al.[16] studied the effect of molecular elongation on deviations of the principle of corresponding states by using first-order perturbation theory. More recently, Monson et al.[17] have determined the phase equilibria of 2CLJ fluids by using second-order perturbation theory. The effect of dipolar forces has also been considered.[18] These studies predicted similar conclusions with respect to the effect of molecular shape on phase equilibria.

Although several simulation studies have been performed for 2CLJ fluids in the liquid region,[19-21] only a few are available concerning the problem of the vapor–liquid equilibria.[22,23] This is mainly due to the fact that the determination of liquid–vapor equilibria by standard simulation techniques requires a large number of simulations. Due to the lack of simulation data of vapor–liquid equilibria of nonspherical models, the predictions on phase equilibria of these perturbation theories could not, in most cases, be compared with simulation results. However, Panagiotopoulos[24] has recently proposed a powerful simulation technique (Gibbs ensemble) for the determination of liquid–vapor equilibria. The Gibbs ensemble simulation method has been used so far in the determination of vapor–liquid equilibria of spherical fluids[24-26] and mixtures of spherical molecule fluids[25,27] and to a few nonspherical models.[28] It is expected that the Gibbs ensemble technique will provide direct liquid–vapor equilibria data so that the predictions of these perturbation theories can be tested.

In the past years several studies concerning Kihara fluids have appeared. Two perturbation theories[11,12] have recently been proposed and a number of simulation studies involving Monte Carlo[29-32] (MC) and molecular dynamics[33] (MD) simulation techniques of linear and nonlinear Kihara models have been performed. The generated computer data in the liquid phase has allowed extensive checking of the perturbation theory proposed by Vega and Lago.[12] This comparison has revealed the main drawback of the theory and an improved version of this perturbation theory has been proposed.[34] This improved perturbation theory agreed very well with the simulation data available for linear and nonlinear models. The results obtained from this improved theory may be considered as satisfactory. However, the determination of liquid–vapor equilibria constitutes a severe test for any theory. In this work we have determined the vapor–liquid equilibria for several linear Kihara molecules using the improved version of the perturbation theory. To check the theoretical results we have performed Gibbs ensemble simulations to determine the liquid–vapor equilibria of these models. A direct comparison between theory and simulation for several linear molecules is then made. The effect of molecular shape on liquid–vapor equilibria is then determined from the theoretical as well as from the simulation results. Deviations from the principle of corresponding states are analyzed.

The scheme of the paper is as follows. In section II we briefly present the perturbation theory. Section III describes the simulation methodology, section IV presents the obtained results, and in section V we present the conclusions of this work.

II. Theory

Two of us have recently proposed[12] a perturbation theory for Kihara (linear or nonlinear molecules). The theory can be regarded as an extension to the Kihara model of the perturbation theory developed by Fischer[7] for nonspherical molecules. This theory is an extension to nonspherical fluids of the well-known perturbation theory developed by Weeks–Chandler–Andersen[35] (WCA) for spherical fluids. We shall briefly describe this perturbation theory of Kihara fluids and refer the reader to refs 12,34 for a more detailed discussion.

The Kihara potential[14] is given by

$$u(\rho) = 4\epsilon\left[\left(\frac{\sigma}{\rho(r,\omega_1,\omega_2)}\right)^{12} - \left(\frac{\sigma}{\rho(r,\omega_1,\omega_2)}\right)^{6}\right] \quad (1)$$

where $\rho(r,\omega_1,\omega_2)$ is the shortest distance between the molecular cores, which hereinafter will be denoted as ρ, ϵ is an energetic parameter, and σ is a size parameter. In the case of linear molecules the natural choice for the molecular core is a rod. Then, ρ is just the shortest distance between the two linear rods (Figure 1). The pair potential $u(\rho)$ is then divided into a reference part $u_0(\rho)$ and a perturbation part $u_1(\rho)$ according to the prescription of Mo and Gubbins[36] so that $u_0(\rho)$ contains all the repulsive forces

* Author to whom correspondence should be addressed.

0022-3654/92/2096-7431$03.00/0

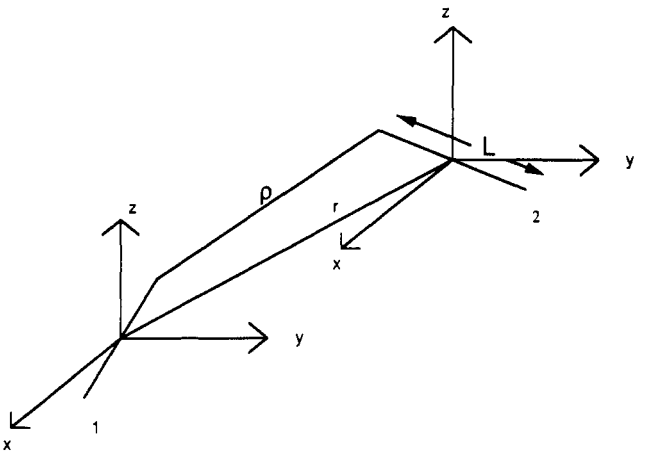

Figure 1. Shortest distance ρ between two linear rods of length L.

and $u_1(\rho)$ all the attractive forces. The residual part of the Helmholtz free energy of the Kihara fluid, A, is now expanded about that of the reference system to obtain up to second order:

$$\frac{A}{NkT} = \frac{A_0}{NkT} + \frac{A_1}{NkT} + \frac{A_2}{NkT} \tag{2}$$

The residual free energy of the reference system A_0 is now set to that of a hard particle with the same length L (Figure 1) and with a diameter d_H. This diameter d_H is obtained at every temperature T and number density n by setting to zero the first-order term of the BLIP expansion[37] of the free energy of the hard particle around that of the reference fluid. The residual free energy of the hard particle is obtained by integrating Boublik's equation of state (EOS) for hard convex bodies.[38,39] With these approximations A_0 is given by

$$A_0 = A_H = \frac{\eta(c_1 + c_2\eta)}{(1-\eta)^2} + c_3 \ln(1-\eta) \tag{3}$$

where the constants c_1, c_2, and c_3 are given by $c_1 = 6\alpha^2 - 2\alpha$, $c_2 = 1.5\alpha(3 - 5\alpha)$, and $c_3 = 6\alpha^2 - 5\alpha - 1$, α being the nonsphericity parameter of the hard particle[39] and η the packing fraction defined as $\eta = nV_H$. Formulas for the evaluation of the volume V_H and of α for hard spherocylinders may be found elsewhere.[39]

To evaluate the perturbation terms A_1 and A_2 in eq 2 the structure of the reference system is needed. To obtain the pair correlation function of the reference system $g_0(r,\omega_1,\omega_2)$ we shall use zero-order RAM theory[40] for the background correlation function of the reference system $y_0(r,\omega_1,\omega_2)$, so that $g_0(r,\omega_1,\omega_2)$ is approximated as

$$g_0(r,\omega_1,\omega_2) = \exp(-\beta u_0(r,\omega_1,\omega_2))y_0(r,\omega_1,\omega_2) \approx \exp(-\beta u_0(r,\omega_1,\omega_2))y_{RAM}(r) \tag{4}$$

where $y_{RAM}(r)$ is the background correlation function of a spherical system interacting through the RAM potential $\Phi_{RAM}(r)$. The RAM potential $\Phi_{RAM}(r)$ is defined by

$$\exp(-\beta\Phi_{RAM}(r)) = \langle \exp(-\beta u_0(r,\omega_1,\omega_2)) \rangle_{12} \tag{5}$$

where the brackets with the subscript 12 stand for unweighted orientational average. The function $y_{RAM}(r)$ is obtained at every temperature and density by solving the Ornstein–Zernike (OZ) equation with the Percus–Yevick (PY) approximation[41] for the potential $\Phi_{RAM}(r)$. The first-order perturbation term A_1 is then given by

$$\frac{A_1}{NkT} = \frac{2n\pi}{kT}\int_0^\infty \langle u_1 \exp(-\beta u_0)\rangle_{12} y_{RAM}(r) r^2 \, dr \tag{6}$$

The second-order perturbation term is obtained from an extension to molecular systems of the macroscopic compressibility equation. The final expression is then[12]

$$\frac{A_2}{NkT} = \frac{-\pi n}{kT}\left(\frac{\partial n}{\partial p}\right)_0 \int_0^\infty \langle u_1^2 \exp(-\beta u_0)\rangle_{12} y_{RAM}(r) r^2 \, dr \tag{7}$$

Equations 2–7 constitute a perturbation theory (PT) for Kihara fluids. In previous work[12,30] we have compared A_0, A_1, and A_2 obtained from PT against their exact values which can be obtained from simulations of the reference system. The main conclusion of these studies is that A_0 and A_2 as given by eqs 3 and 7, respectively, agree very well with simulation results. A_1 from PT agrees well with the simulation results at low densities and small anisotropies. However, as the molecular anisotropy and/or the density increase the theoretical prediction of A_1 becomes worse. These conclusions hold for linear and nonlinear Kihara molecules. The deviations in A_1 between theoretical and simulation results have a significant effect on the calculated thermodynamic properties of the Kihara fluid.[34] To make the theory a useful tool for the prediction of the phase diagram and EOS of Kihara fluids, an improvement in the determination of A_1 is required. From a purely theoretical point of view this improvement requires the substitution of $y_{RAM}(r)$ in eq 4 by some function which incorporates some orientational dependence, and work should be done in that direction. However, we have recently shown that the deviations ΔA_1 between calculated A_1 and exact $A_1^{simulation}$ values show a smooth behavior as a function of both density and anisotropy and may be fitted to an empirical expression:[34]

$$\Delta A_1 = 100\frac{(A_1^{simulation} - A_1)}{A_1^{simulation}} \tag{8}$$

$$\Delta A_1 = (185.52\alpha - 188.42)(\eta - 0.12) \qquad \alpha > 1.03 \; \eta > 0.12 \tag{9}$$

$$\Delta A_1 = 0 \qquad \text{otherwise} \tag{10}$$

Equations 8–10 allow us to correct the theoretical values of the first order perturbation term A_1 obtained from eq 6. When the A_1 term is corrected in this way we obtain an improved perturbation theory (IPT). Although the IPT possesses some empirical character, it has proved to be in very good agreement with simulation results for several Kihara models in a wide range of temperatures and densities.[34] Thus, some confidence in the ability of the IPT theory to describe the liquid region of Kihara fluids has been gained. Its capacity to predict correctly the vapor–liquid equilibria will be analyzed in this work.

The liquid–vapor equilibria of Kihara fluids was determined from the IPT theory as follows. For $T/T_c < 0.8$, where T_c stands for the critical temperature, the densities of the vapor in equilibrium with the liquid are very small. Thus, we used IPT to describe the liquid phase while the gas phase was described with the second virial coefficient. The liquid–vapor equilibria was then obtained by equating the pressure and chemical potential in both phases. For higher temperatures ($T/T_c > 0.8$) we used IPT theory for both the liquid and the vapor and phase equilibria was determined in the G,p diagram. The critical temperature and density obtained from the IPT theory which we call T_c^{IPT} and n_c^{IPT} were obtained by fitting the theoretical bubble and dew densities at high temperatures to the expressions

$$(n_l + n_g)/2 = s_1 + s_2 T + s_3 T^2 \tag{11}$$

$$n_l - n_g = d_1\left(1 - \frac{T}{T_c}\right)^{1/2} + d_2\left(1 - \frac{T}{T_c}\right) + d_3\left(1 - \frac{T}{T_c}\right)^2 \tag{12}$$

Equation 11 is the law of the rectilinear parameters (except for the quadratic term). The first term on the right-hand side of eq 12 was used so that the fit guarantees the classical exponent ($\beta = 1/2$) obtained from the theory.[42] We fitted the theoretical vapor pressures to the Antoine's equation,[43] and then by extrapolation to the critical temperature T_c^{IPT} the theoretical critical pressure p_c^{IPT} was determined.

In the next section we present the simulation methodology followed to determine the liquid–vapor equilibria of Kihara fluids.

III. Simulation Methodology

To determine the liquid–vapor equilibria of linear Kihara molecules we shall use the Gibbs ensemble Monte Carlo (MC)

simulation technique. This method was developed by Panagiotopoulos[24] for pure fluids and allows a direct determination of the liquid–vapor equilibria. It has been applied to several spherical models and extended to mixtures.[24-27] The method may be used to determine liquid–vapor equilibria of nonspherical particles as well. In fact it has recently been used to obtain the liquid–vapor equilibria of linear Gay–Berne models.[28] The Gibbs ensemble technique involves three different steps. In the first one, a conventional NVT MC simulation[44] is performed in the liquid and in the vapor. In the second step, an attempt is made to change the volume of one simulation box by ΔV and the other simulation box by $-\Delta V$. The prescription for the acceptance of the global move is taken from the NPT MC simulation assuming equal pressures for the liquid and vapor phases. However, in contrast with the conventional NPT MC method there is no need to specify the equilibrium pressure at the beginning of the simulation. The third step consists of a particle exchange. A particle in one of the boxes (liquid or vapor) is destroyed and inserted with a random position and orientation in the other box. The trial move is accepted with a probability taken from the μVT MC simulation[44] assuming equal chemical potential in both phases. Again, it is not necessary to specify the value of the chemical potential at the beginning of the run. For a more detailed description of the method we refer the reader to the original papers.[24,25]

The details of our simulations are close to those of ref 28. We used 512 particles in all cases. In the original configuration we set 256 particles in the liquid and 256 particles in the gas phase in an α-N_2 lattice.[44] The values of the initial densities of the liquid and gas were taken from the perturbation theory described in the previous section (IPT). That makes the equilibration period considerably shorter. Nevertheless, for some cases we considered other sets of initial densities and obtained identical results. A run typically consist of 2000–3000 cycles for equilibration followed by 3000–7000 cycles for obtaining averages. A cycle consists of an attempt at moving each particle in the liquid simulation box and then in the gas simulation box, followed by an attempt at changing the volume, and finally N_{ex} attempts exchanging particles between the simulation boxes. The acceptance ratio in the standard NVT MC and in the volume change was kept in the range 30–50%. The number N_{ex} was chosen according to Panagiotopoulos prescription[24] so that 1–3% of the particles were exchanged in each cycle.

The pair potential was truncated at $\rho_c = 3\sigma$. However, as indicated in ref 25, the long-range corrections were included in the steps involving a volume change or a particle exchange since these moves involve a change in the density of the system. The long-range corrections were obtained by assuming uniform fluid beyond the cutoff. Formulas for the evaluation in Kihara fluids of the long-range contribution to thermodynamic properties may be found in ref 29.

The evaluation of the pair potential (see eq 1) requires the calculation of the shortest distance between two linear rods ρ and algorithms for its determination are available elsewhere.[45,46]

We typically studied the vapor–liquid equilibria with the Gibbs ensemble for $T/T_c > 0.70$. The critical temperature T_c^{MC} and density n_c^{MC} were estimated by fitting the bubble and dew densities to the expressions:[47]

$$(n_l + n_g)/2 = s_1 + s_2 T \tag{13}$$

$$n_l - n_g = d_1\left(1 - \frac{T}{T_c}\right)^{1/3} \tag{14}$$

The critical pressure p_c^{MC} was obtained by extrapolating to T_c^{MC} an empirical fit to the MC vapor pressures (as obtained from the virial theorem in the vapor phase). We were not able to use the Gibbs ensemble for the determination of the phase equilibria when $T/T_c < 0.70$. The reason was that for low temperatures the density of the liquid is very high and the probability of inserting/removing a particle becomes very small. Therefore, a huge number of exchange attempts N_{ex} is required to guarantee an 1–3% exchange of particles and that makes the simulation prohibitively time consuming. Möller and Fischer[48] using the NpT + test particle method were able to obtain the liquid–vapor equilibria for 2CLJ with $L^* = 0.505$ at $T/T_c = 0.70$. In any case it seems clear that the insertion in a dense system becomes more difficult as the molecular anisotropy increases. At low temperatures we have therefore followed a different approach. Instead of determining the liquid–vapor equilibria, we have determined the zero-pressure density at two different temperatures (about $T/T_c = 0.5$ and $T/T_c = 0.6$) from NVT MC simulations. Since the vapor pressure is very small at these low temperatures, the bubble density and the zero-pressure density should be very close. The details of these MC (NVT) simulations are given in refs 29 and 30. We used 256 particles with 3000 cycles for equilibration followed by 4000 cycles to obtain thermodynamical averages.

We have studied three different Kihara linear fluids with anisotropies $L^* = L/\sigma = 0.3$, 0.6, and 0.8. For $T/T_c > 0.7$ we used the Gibbs ensemble technique and from these results the critical point was estimated. For $T/T_c = 0.5$,0.6 we determined the zero-pressure densities and identified them with the bubble densities.

TABLE I: Gibbs Ensemble Results for $L^* = 0.30$[a]

T^*	n_g^*	p_g^*	n_l^*	p_l^*
1.100	0.114 (8)	0.067 (4)	0.317 (28)	0.066 (17)
1.100	0.118 (10)	0.067 (5)	0.295 (43)	0.062 (19)
1.085	0.115 (8)	0.064 (4)	0.337 (21)	0.063 (14)
1.075	0.107 (8)	0.059 (4)	0.367 (21)	0.064 (21)
1.050	0.086 (3)	0.053 (2)	0.375 (15)	0.061 (21)
1.025	0.077 (7)	0.048 (2)	0.399 (13)	0.046 (31)
1.000	0.063 (5)	0.041 (2)	0.421 (9)	0.043 (9)
1.000	0.057 (4)	0.039 (2)	0.415 (12)	0.038 (30)
0.975	0.044 (2)	0.032 (1)	0.428 (12)	0.035 (29)
0.95	0.041 (1)	0.029 (1)	0.445 (12)	0.033 (32)
0.90	0.028 (1)	0.020 (1)	0.470 (8)	0.020 (45)
0.90	0.029 (1)	0.021 (1)	0.474 (9)	0.031 (42)
0.90	0.030 (1)	0.021 (1)	0.474 (11)	0.026 (81)
0.85	0.018 (2)	0.013 (1)	0.492 (9)	0.012 (29)
0.85	0.019 (1)	0.014 (1)	0.497 (8)	0.020 (43)
0.80	0.012 (1)	0.009 (1)	0.516 (8)	0.002 (34)
0.80	0.012 (1)	0.008 (1)	0.514 (7)	0.000 (49)
0.70[b]			0.563	0.000
0.60[b]			0.592	0.000

[a] The results are given in reduced units, $L^* = L/\sigma$, $T^* = T/(\epsilon/k)$, $n^* = n\sigma^3$, and $p^* = p/(\epsilon/\sigma^3)$. The number in parentheses is the accuracy of the last decimal(s), so 0.375 (15) means 0.375 ± 0.015. The estimated errors were obtained from the standard deviation over blocks of length 100 cycles. The last two rows correspond to the zero pressure densities as estimated from the NVT simulations of Table IV. [b] Zero-pressure densities obtained from NVT simulations (see Table IV).

IV. Results and Discussion

The three studied elongations ($L^* = 0.3$, 0.6, 0.8) correspond approximately to the molecular anisotropy presented by N_2, Cl_2, and CO_2, respectively. For $L^* = 0.0$ the linear Kihara model reduces to the spherical Lennard-Jones (12-6) potential for which MC results for the vapor–liquid equilibria are available.[24-26] By changing L^* from 0 to 0.8 we can analyze the changes that the vapor–liquid equilibrium undergoes when going from a spherical molecule to a molecule with a CO_2 like anisotropy.

In Tables I–III the results of the Gibbs ensemble simulations are presented. We present the pressure as obtained from the virial theorem for the liquid and vapor phases. They mutually agree within the error of the simulations. However, the vapor pressure obtained in the vapor phase is affected by a considerably smaller error bar. We used these values to estimate the critical pressure. For a number of states we have done two independent runs differing in the initial conditions. In general, the results of these independent runs agree within the statistical error. In Table IV we present the results of the NVT MC runs. The zero-pressure densities were obtained by linear interpolation (extrapolation) and are shown in the last two rows of Tables I–III. The results of Tables I–III cover almost entirely the liquid–vapor equilibria range since they go from the critical to the proximities of the triple point (approximately $T/T_c = 0.50$). Therefore, they constitute a severe test for any theory.

TABLE II: As in Table I for $L^* = 0.60$

T^*	n_g^*	p_g^*	n_l^*	p_l^*
1.000	0.114 (36)	0.048 (7)	0.166 (24)	0.050 (7)
0.990	0.097 (19)	0.046 (6)	0.224 (33)	0.045 (11)
0.975	0.094 (8)	0.044 (3)	0.256 (25)	0.041 (15)
0.950	0.068 (4)	0.037 (2)	0.287 (20)	0.039 (17)
0.950	0.064 (5)	0.036 (3)	0.290 (16)	0.036 (25)
0.925	0.045 (2)	0.028 (2)	0.299 (12)	0.026 (19)
0.900	0.039 (1)	0.024 (2)	0.316 (10)	0.022 (28)
0.875	0.030 (1)	0.020 (1)	0.331 (7)	0.012 (22)
0.850	0.024 (1)	0.016 (1)	0.342 (7)	0.006 (36)
0.800	0.017 (1)	0.011 (1)	0.365 (7)	0.000 (41)
0.750	0.011 (1)	0.007 (1)	0.389 (5)	−0.002 (36)
0.710	0.007 (1)	0.004 (1)	0.403 (5)	0.008 (65)
0.675	0.0049 (3)	0.0030 (2)	0.413 (6)	0.001 (34)
0.65[a]			0.424	0.000
0.55[a]			0.454	0.000

[a] Zero-pressure densities obtained from NVT simulations (see Table IV).

TABLE III: As in Table I for $L^* = 0.80$

T^*	n_g^*	p_g^*	n_l^*	p_l^*
0.940	0.091 (5)	0.038 (4)	0.211 (24)	0.040 (16)
0.935	0.082 (6)	0.036 (4)	0.213 (21)	0.036 (12)
0.930	0.069 (6)	0.034 (3)	0.208 (26)	0.033 (12)
0.920	0.064 (3)	0.032 (2)	0.237 (14)	0.033 (16)
0.910	0.049 (4)	0.028 (2)	0.230 (17)	0.023 (12)
0.900	0.044 (3)	0.026 (1)	0.247 (13)	0.026 (14)
0.900	0.049 (3)	0.027 (1)	0.240 (14)	0.028 (15)
0.875	0.035 (2)	0.022 (1)	0.256 (10)	0.022 (15)
0.850	0.029 (1)	0.019 (1)	0.279 (5)	0.018 (14)
0.850	0.028 (1)	0.018 (1)	0.272 (13)	0.013 (21)
0.825	0.025 (1)	0.015 (1)	0.290 (9)	0.013 (23)
0.800	0.019 (1)	0.012 (1)	0.300 (8)	0.012 (21)
0.800	0.019 (1)	0.012 (1)	0.301 (6)	0.014 (23)
0.75	0.013 (1)	0.008 (1)	0.324 (7)	0.010 (22)
0.70	0.008 (1)	0.005 (1)	0.339 (5)	0.007 (20)
0.650	0.0047 (2)	0.0028 (1)	0.357 (3)	0.002 (25)
0.60[a]			0.372	0.000
0.50[a]			0.399	0.000

[a] Zero-pressure densities obtained from NVT simulations (see Table IV).

TABLE IV: Equation of State of Linear Kihara Fluids As Obtained from NVT Monte Carlo Simulations[a]

L^*	T^*	n^*	$Z = p/(nkT)$
0.30	0.60	0.570	−0.977
0.30	0.60	0.585	−0.312
0.30	0.70	0.530	−0.617
0.30	0.70	0.550	−0.240
0.60	0.55	0.445	−0.623
0.60	0.55	0.465	0.737
0.60	0.65	0.40	−0.676
0.60	0.65	0.42	−0.109
0.80	0.50	0.38	−1.375
0.80	0.50	0.40	0.090
0.80	0.60	0.35	−0.845
0.80	0.60	0.37	−0.072

[a] These results were used to estimate the zero-pressure densities shown in the last two rows of Tables I–III. Units as in Table I.

In Figure 2 we compare the coexistence densities obtained from simulation with those obtained from the perturbation theory (IPT) described in section II. The agreement is remarkably good. The deviations between the theoretical and simulation bubble densities are smaller than 3% from the triple point up to $T/T_c = 0.90$. Moreover, the quality of the results does not deteriorate when increasing the molecular anisotropy from $L^* = 0.30$ to $L^* = 0.80$. At low temperatures, the theory slightly underestimates the bubble densities for all the elongations. However, for temperatures above $T/T_c = 0.90$ the theory deviates significantly from the simulation results. These deviations are expected since at temperatures close to the critical point the convergence of the perturbation expansion

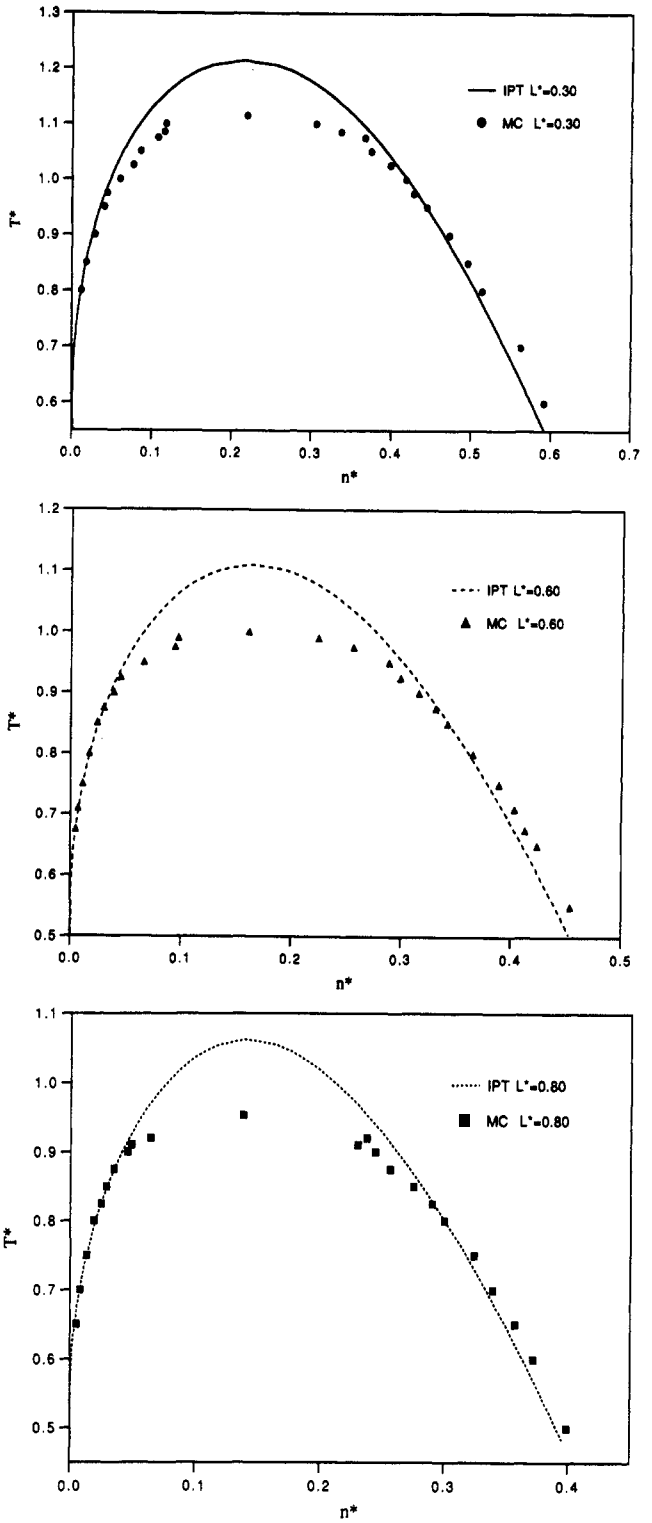

Figure 2. Vapor–liquid coexistence densities for Kihara fluids. The results are in reduced units $T^* = T/(\epsilon/k)$ and $n^* = n\sigma^3$. The lines correspond to the results of the perturbation theory (IPT) and the markers to the simulation results. (a) Results for $L^* = L/\sigma = 0.30$. (b) Results for $L^* = 0.60$. (c) Results for $L^* = 0.80$.

deteriorates and a second-order treatment is probably insufficient. Moreover, the theory predicts classical exponents[42] ($\beta = 1/2$) and that should yield a higher critical temperature. More theoretical work on fluids at medium densities and in the proximity of the critical point is needed. Figure 3 presents the liquid branch of the vapor–liquid equilibria for $L^* = 0$, 0.3, 0.6, 0.8 as determined from theory and from simulation. We conclude that the IPT theory constitutes a reliable tool to determine liquid–vapor coexistence densities of linear Kihara fluids from spherical to highly nonspherical (CO_2 like) models.

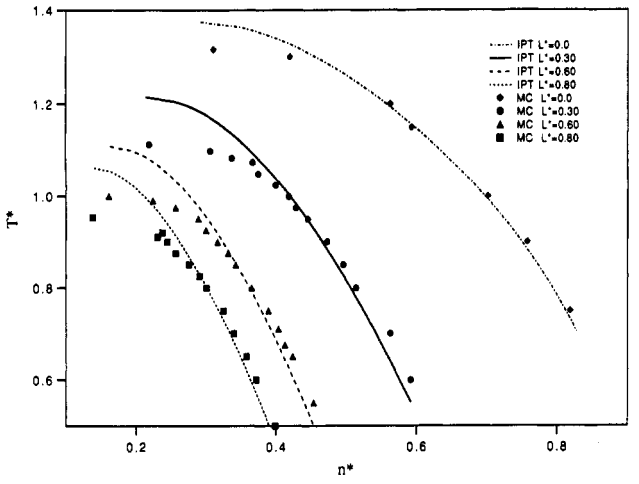

Figure 3. Bubble densities as obtained from perturbation theory (lines) and from simulation (markers) for (from top to bottom) $L^* = 0$, 0.3, 0.6, and 0.80.

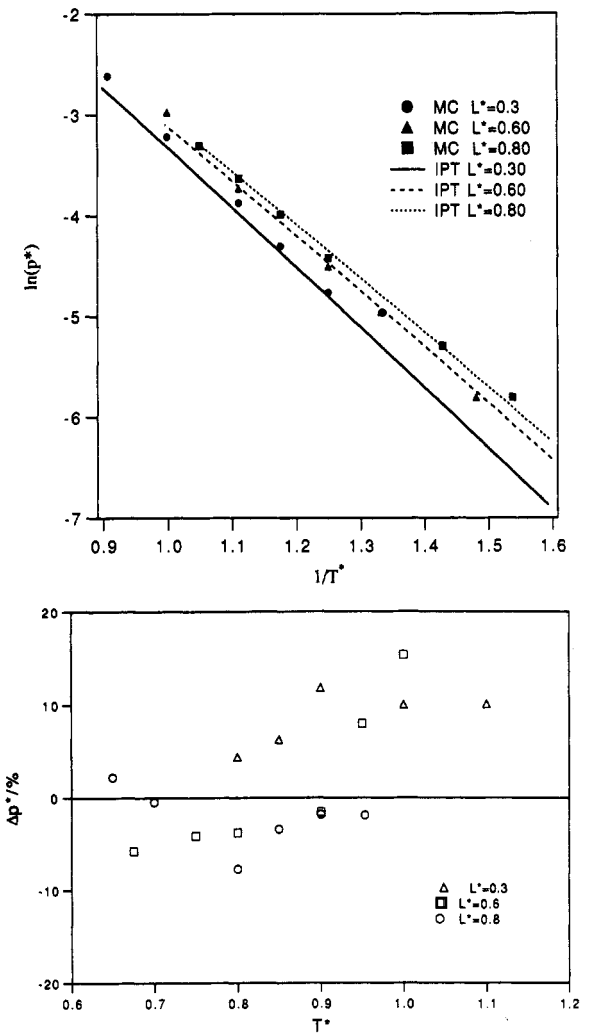

Figure 4. (a) Vapor pressures ($p^* = p/(\epsilon/\sigma^3)$) as obtained from perturbation theory (lines) and from simulation (markers) for linear Kihara fluids. The results correspond (from the top to the bottom) to $L^* = 0.80$, 0.60 and 0.30. (b) Deviation plot of the MC vapor pressures (markers) with respect to the IPT results.

Another interesting property is the vapor pressure. Since this property typically changes several orders of magnitude over the coexistence curve it is especially sensitive to the approximations made in any theoretical treatment. In Figure 4a we show the vapor pressure as obtained from the simulation and from the theory. The agreement is again good for the three studied models. At high temperatures ($T/T_c > 0.90$) there are discrepancies between calculated (IPT) and observed (MC) vapor pressures, although the differencies are not so large as those found in the determination of the coexistence densities. The IPT theory may be used to obtain reasonable estimates of the vapor pressure in the temperature range $T/T_c = 0.9$ to $T/T_c = 1$. Between $T/T_c = 0.7$ and $T/T_c = 0.90$ the theory (IPT) provides reliable results. Unfortunately, we could not check our theoretical results for $T/T_c < 0.70$ since, as already pointed out, we were not able to use the Gibbs ensemble technique successfully at low temperatures. For $L^* = 0.30$ the theoretical vapor pressures are low by about 8%. We believe this is due to the use of second-order perturbation theory which tends in the case of quasi-spherical models to underestimate vapor pressure whereas first-order perturbation theory[16,49] tends to overestimate it. In Figure 4b we show the deviations between the theoretical vapor pressures (IPT) and the ones obtained from simulation. The average deviation for the vapor pressures between the theoretical and the MC results is about 6%. The average uncertainty of the MC vapor pressures is of about 7%. We conclude that IPT constitutes a reliable tool for the prediction of vapor–liquid equilibria of Kihara fluids. It should be pointed out that the former PT systematically underestimates the bubble densities and overestimates the vapor pressures in the case of Kihara fluids. For instance, for $L^* = 0.60$ the bubble densities are about 7% smaller than the MC values whereas the vapor pressures are about 30% too high. The improvement of the IPT over the PT version is quite significant for medium and large elongations.

TABLE V: Critical Point of Linear Kihara Fluids As Estimated from the Gibbs Ensemble Results of This Work (MC) and from the Improved Perturbation Theory (IPT)[a]

MC

L^*	T_c^{MC}	n_c^{MC}	p_c^{MC}	η_c^{MC}
0.00[b]	1.316	0.310	0.130	0.162
0.30	1.114 (12)	0.219 (6)	0.073 (10)	0.166 (5)
0.60	1.000 (12)	0.161 (5)	0.051 (10)	0.160 (5)
0.80	0.952 (11)	0.140 (3)	0.038 (8)	0.161 (4)

IPT

L^*	T_c^{IPT}	n_c^{IPT}	p_c^{IPT}	η_c^{IPT}
0.00	1.375	0.292	0.166, 0.095[d]	0.153
0.30	1.215	0.214	0.103, 0.066[d]	0.162
0.60	1.110	0.164	0.075, 0.045[d]	0.163
0.60[c]	1.144	0.165	0.078, 0.044[d]	0.164
0.80	1.063	0.141	0.065, 0.038[d]	0.162
1.20	0.986	0.113	0.057	0.166

[a] The results are given in reduced units (see Table I). The packing fraction at the critical point η_c is given by $\eta_c = n_c V$, where V is the volume of a hard spherocylinder of elongation L^*. The MC estimates of the critical density and temperature for $L^* = 0.0$ (Lennard-Jones) were taken from ref 50 whereas the critical pressure was estimated from the results of ref 25. [b] Results from ref 50. [c] The results of this row correspond to IPT theory used to first order. [d] Vapor pressure from IPT at $T = T_c^{MC}$.

We now turn to analyzing the effect of molecular anisotropy on critical properties. Table V shows the critical properties (density, pressure, and temperature) as estimated from the simulation results (MC) and from the perturbation theory (IPT). First, we see that the molecular anisotropy decreases the critical properties and this kind of behavior is predicted by both the theory and the simulation results. This is more clearly illustrated in Figure 5a. The critical temperature decreases steeply at small elongations and more smoothly as the elongation increases. In the Kihara model the value of the well depth ϵ does not depend on the molecular elongation or on the relative orientation. The meaning of the decrease in the critical temperature with the elongation is that when two molecules of different anisotropy interact with the same energy (ϵ) the one with the highest anisotropy will have the smallest critical temperature. The decrease in the critical temperature and density as a function of molecular elongation has also been observed[16,17,23] for the two-center Lennard-Jones model (2CLJ) and for Gay–Berne fluids.[28] The trends

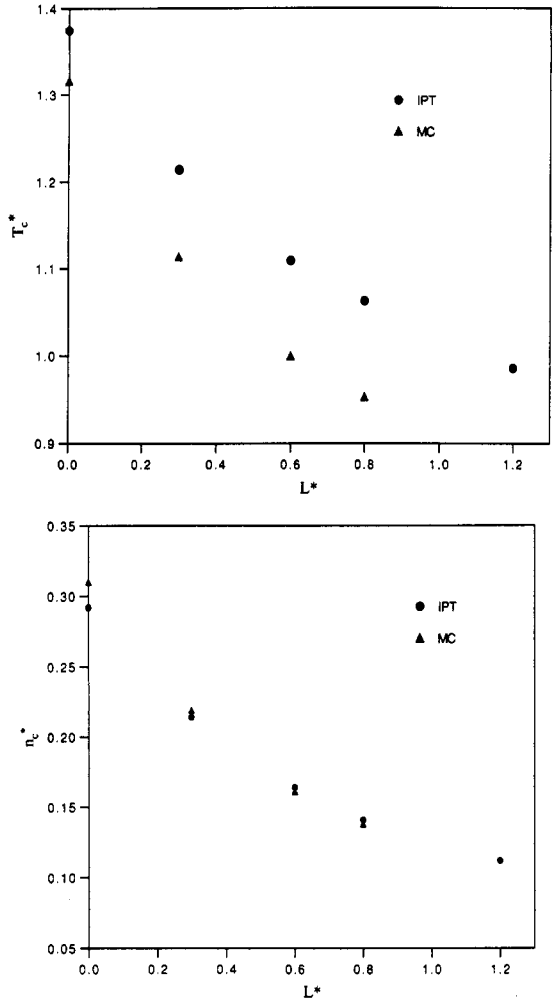

Figure 5. Critical properties of linear Kihara molecules as a function of the elongation L^*. The circles correspond to the critical values from perturbation theory (IPT) and the triangles correspond to the estimate of the critical properties from the Gibbs ensemble simulation. (a) Results for the critical temperature. (b) Results for the critical density.

found for the critical properties of the Kihara model are close to those of 2CLJ. The values of the critical temperature obtained from IPT are significantly higher than those estimated from the MC results. The ratio of T_c^{IPT}/T_c^{MC} is about 1.10 in all the cases. For the 2CLJ fluid, Fischer et al.[16] found a ratio of the theoretical critical point to that of some real substances of about 1.15. More recently, Monson et al.[17] found for the 2CLJ this ratio to be about 1.07 by using a different perturbation scheme. Our results show the same kind of deviation. For $L^* = 0.6$, we have also estimated the critical point by using IPT theory but only to first order (neglecting the second-order term). As can be seen in Table III, the critical temperature from second-order perturbation theory is closer (although still in poor agreement) to the MC value than the one from first-order perturbation theory.

Table V shows the critical density as estimated from the MC results and from the theory (IPT). Figure 5b shows the variation of the critical density with the molecular elongation. The agreement between the theoretical and estimated (MC) critical densities is very good. The IPT can therefore be used to obtain a reasonable estimation of the critical densities. In the reduced units $n^* = n\sigma^3$, the critical densities decrease as the molecular elongation increases. This is due to the fact that the molecular volume increases with the molecular elongation L^*. However, when the packing fraction (the fraction of space occupied by the molecules) is calculated at the critical point it turns out that it is nearly constant and in the range 0.16–0.17 for all the analyzed models.

The critical pressures as estimated from (MC) and determined from the theory (IPT) are also shown in Table V. The theoretical

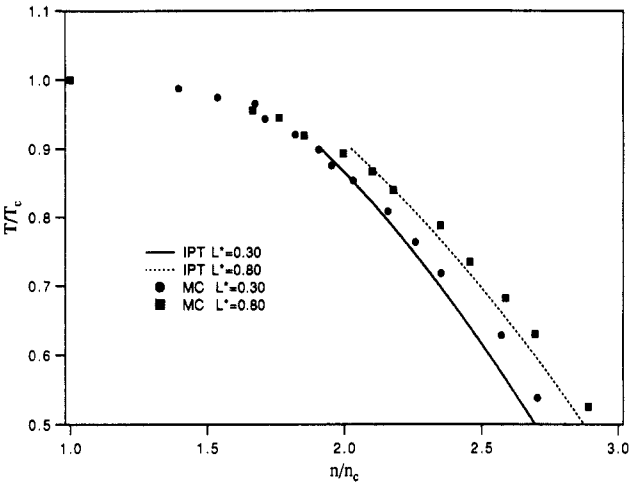

Figure 6. Reduced bubble densities as a function of the reduced temperature for $L^* = 0.30$ and $L^* = 0.80$. T_c and n_c stand for the critical temperature and density, respectively, as estimated from the Gibbs ensemble simulations of this work. The lines correspond to the bubble densities from perturbation theory (IPT) and the markers are the bubble densities from the MC results.

critical pressures are too high due to the overestimation of the critical temperatures. When the theoretical vapor pressures are calculated at T_c^{MC}, they agree better with p_c^{MC} (see Table V). The critical pressure decreases as the molecular elongation increases.

From the results presented so far it may be concluded that molecular shape has a great effect on vapor–liquid coexistence and on critical properties. This is also what is observed in real fluids. However, Gugenheim[47] has shown that when the coexistence properties are scaled by the respective critical values, many fluids obey very closely the same behavior law. This is known as the principle of corresponding states. Noble gases such as argon, krypton, or xenon conform very well to the principle of corresponding states. This is because all of them possess spherical symmetry. Molecules with a mild anisotropy such as N_2 or O_2 present almost the same behavior (in scaled units) as spherical molecules. However, when the molecular anisotropy increases, it has been experimentally found that the reduced coexistence properties deviate significantly from the behavior found for spherical molecules. Now we shall analyze our results to study deviations from the principle of corresponding states due to molecular shape.

In Figure 6 we show the orthobaric densities as obtained from IPT and from MC for $L^* = 0.3$ and $L^* = 0.80$. We have reduced the results by using the critical properties estimated from the MC results (see Table V) which are the most reliable estimations of the critical properties available at present for these models. The molecular anisotropy increases the reduced density for a given reduced temperature when both magnitudes are reduced by their critical values. This is predicted by both the theoretical and the simulation results. However, the effect, although noticeable, is moderate. For example, at $0.5T_c$ the reduced density increases about 7% when the molecular anisotropy is changed from $L^* = 0.30$ (N_2 like) to $L^* = 0.80$ (CO_2 like). Real substances behave in this way. For example, the reduced densities at $0.5T_c$ for argon, ethane, propane, and isobutane take the values 2.75, 2.85, 2.90, and 2.95, respectively. Two previous theoretical studies of the 2CLJ model[16,17] also found an increase in the reduced densities at a given reduced temperature as the molecular anisotropy increases. Here we present more evidence to support this argument, using both theory and simulation and a different potential model. We conclude that molecular anisotropy provokes an increase in bubble densities at a given temperature when both are scaled in critical units. It should however be remembered that here we are considering shape effects only. To study real molecules the effect of polarity (dipolar or quadrupolar moments) should be included.

Now we analyze the deviations from the principle of corresponding states for the vapour pressure. In Figure 7 we show the

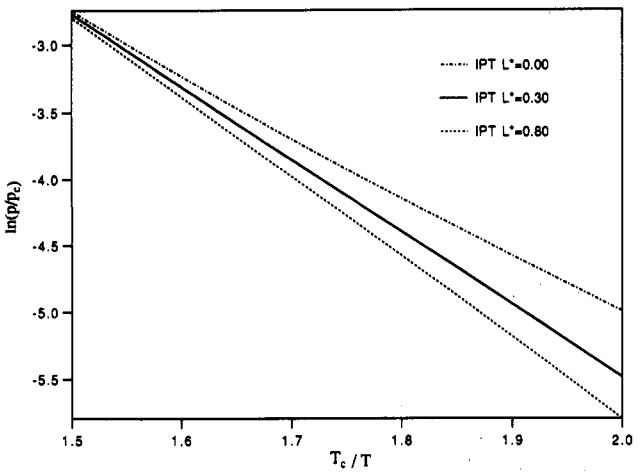

Figure 7. Reduced vapor pressures as a function of the reduced temperature for $L^* = 0$, 0.3, and 0.80. T_c and p_c stand for the critical temperature and pressure, respectively, as estimated from Gibbs ensemble simulations (see Table V). The lines correspond to the vapor pressures from perturbation theory (IPT).

vapor pressure as a function of the inverse of the temperature for $L^* = 0.00$, $L^* = 0.30$, and $L^* = 0.80$. We show the vapor pressures as obtained from the IPT theory and scaled by the best estimation of the critical properties of the models available at present (MC values of Table V). The molecular anisotropy considerably decreases (it becomes more negative) the slope of the vapor pressure curve as a function of the inverse of the temperature. Note the logarithmic scale on the ordinates axes. The deviations are quite important. At $T/T_c = 0.50$ the deviations in the vapor pressure in reduced units between $L^* = 0.30$ and $L^* = 0.80$ are about 30%. The effect of molecular anisotropy on deviations from the principle of corresponding states seems to be more pronounced for vapor pressures than for bubble densities. The molecular anisotropy increases the steepness of the vapor pressure curve with respect to that of a spherical fluid. The same conclusion was obtained by Fischer et al.[16] and Monson et al.[17] from their perturbation theories for the 2CLJ model. This kind of behavior is also found experimentally and is the basis of the definition of the acentric factor.[51]

V. Conclusions

The critical temperatures and pressures of linear Kihara fluids decreases with molecular elongation while the critical packing fraction takes an almost constant value of about 0.165. The liquid–vapor coexistence properties of linear Kihara fluids for temperatures up to $T/T_c = 0.90$ can be obtained with a great degree of accuracy with a recently proposed perturbation theory[12,34] of Kihara fluids. The theory provides good estimates of the critical densities but systematically overpredicts the critical temperature and pressure. More theoretical work on fluids at medium densities is therefore needed. The molecular anisotropy provokes deviations from the principle of corresponding states. When scaled by the critical values, the anisotropy increases the bubble density and reduces the vapor pressure at a given temperature. This is also what is found in real fluids. The trends with molecular elongation of Kihara fluids found in this work are the same as those found for the two-center Lennard-Jones model as determined from two previous theoretical studies.[16,17]

Acknowledgment. This work has been financially supported by project PB88-0143 of the CAICYT and by project PB89-0640 of the Consejeria de Educacion y Ciencia de la Junta de Andalucia. Generous allocation of computer time at the Centro Informatico Cientifico de Andalucia (CICA) is greatly acknowledged.

References and Notes

(1) Gray, C. G.; Gubbins, K. E. *Theory of Molecular Fluids*; Claredon: Oxford, U.K., 1984.
(2) Lee, L. L. *Molecular Thermodynamics of Nonideal Fluids*; Butterworth Publishers: Stoneham, U.K., 1987.
(3) Lado, F. *Mol. Phys.* **1982**, *47*, 283.
(4) Lomba, E.; Lombardero, M.; Abascal, J. L. F. *J. Chem. Phys.* **1989**, *91*, 2581.
(5) Perera, A.; Patey, G. N. *J. Chem. Phys.* **1987**, *87*, 1295.
(6) Lago, S.; Sevilla, P. *J. Chem. Phys.* **1988**, *89*, 4349.
(7) Fischer, J. *J. Chem. Phys.* **1980**, *72*, 5371.
(8) Tildesley, D. J. *Mol. Phys.* **1980**, *41*, 341.
(9) Lombardero, M.; Abascal, J. L. F.; Lago, S. *Mol. Phys.* **1981**, *42*, 999.
(10) Lupkowski, M.; Monson, P. A. *J. Chem. Phys.* **1987**, *87*, 3618.
(11) Boublik, T. *J. Chem. Phys.* **1987**, *87*, 1751.
(12) Vega, C.; Lago, S. *J. Chem. Phys.* **1991**, *94*, 310.
(13) Gubbins, K. E.; Twu, C. H. *Chem. Eng. Sci.* **1979**, *33*, 863.
(14) Kihara, T. *J. Phys. Soc. Jpn.* **1951**, *16*, 289.
(15) Berne, B. J.; Pechukas, P. *J. Chem. Phys.* **1972**, *56*, 4213.
(16) Fischer, J.; Lustig, R.; Breitenfelder-Manske, H.; Lemmin, W. *Mol. Phys.* **1984**, *52*, 485.
(17) McGuigan, D. B.; Lupkowski, M.; Paquet, D. M.; Monson, P. A. *Mol. Phys.* **1989**, *67*, 33.
(18) Lupkowski, M.; Monson, P. A. *Mol. Phys.* **1989**, *67*, 53.
(19) Streett, W. B.; Tildesley, D. J. *Proc. R. Soc. London A* **1977**, *355*, 239.
(20) Romano, S.; Singer, K. *Mol. Phys.* **1979**, *37*, 1765.
(21) Wojcik, M.; Gubbins, K. E. *Mol. Phys.* **1982**, *45*, 1209.
(22) Powles, J. G. *Mol. Phys.* **1980**, *41*, 715.
(23) Gupta, S. *J. Phys. Chem.* **1988**, *92*, 7156.
(24) Panagiotopoulos, A. Z. *Mol. Phys.* **1987**, *61*, 813.
(25) Panagiotopoulos, A. Z.; Quirke, N.; Stapleton, M.; Tildesley, D. J. *Mol. Phys.* **1988**, *63*, 527.
(26) Smit, B.; De Smedt PH; Frenkel, D. *Mol. Phys.* **1989**, *68*, 931. Smit, B.; Frenkel, D. *Mol. Phys.* **1989**, *68*, 951. Rudsill, E. N.; Cummings, P. T. *Mol. Phys.* **1989**, *68*, 629.
(27) Harismiadis, V. I.; Koutras, N. K.; Tassios, D. P.; Panagiotopoulos, A. Z. *Fluid Phase Equilib.* **1991**, *65*, 1.
(28) De Miguel, E.; Rull, L. F.; Chalam, M. K.; Gubbins, K. E. *Mol. Phys.* **1990**, *71*, 1223. De Miguel, E.; Rull, L. F.; Gubbins, K. E. *Physica A* **1991**, *177*, 174.
(29) Vega, C.; Frenkel, D. *Mol. Phys.* **1989**, *67*, 633.
(30) Vega, C.; Lago, S. *Mol. Phys.* **1991**, *72*, 215.
(31) Kantor, R.; Boublik, T. *Czech. J. Phys.* **1988**, *B38*, 321.
(32) Kantor, R.; Boublik, T. *Mol. Simul.* **1989**, *2*, 217.
(33) Vega, C.; Lago, S. *J. Chem. Phys.* **1990**, *93*, 8171.
(34) Vega, C.; Lago, S. *Chem. Phys. Lett.* **1991**, *185*, 516.
(35) Weeks, J. D.; Chandler, D.; Andersen, H. C. *J. Chem. Phys.* **1971**, *54*, 5237.
(36) Mo, K. C.; Gubbins, K. E. *Chem. Phys. Lett.* **1974**, *27*, 144.
(37) Hansen, J. P.; McDonald, I. R. *Theory of Simple Liquids*, 2nd ed.; Academic Press: New York, 1986.
(38) Boublik, T. *Mol. Phys.* **1981**, *42*, 209.
(39) Boublik, T.; Nezbeda, I. *Collect. Czech. Chem. Commun.* **1986**, *51*, 2301.
(40) Smith, W. R.; Nezbeda, I. *Adv. Chem. Ser.* **1983**, *204*, 235.
(41) Percus, J. K.; Yevick, G. J. *Phys. Rev.* **1958**, *110*, 1.
(42) Rowlinson, J. S.; Swinton, F. L. *Liquids and Liquid Mixtures*; Butterworth: London, 1982.
(43) Reid, R. C.; Prausnitz, J. M.; Poling, B. E. *The Properties of Gases and Liquids*; McGraw-Hill: New York, 1987.
(44) Allen, M. P.; Tildesley, D. J. *Computer Simulation of Liquids*; Clarendom Press: Oxford, U.K., 1987.
(45) Sevilla, P.; Lago, S. *Comput. Chem.* **1985**, *9*, 39.
(46) Lago, S.; Vega, C. *Comput. Chem.* **1988**, *12*, 343.
(47) Guggenheim, E. A. *J. Chem. Phys.* **1945**, *13*, 253.
(48) Möller, D.; Fischer, J. *Mol. Phys.* **1990**, *69*, 463.
(49) Lotfi, A.; Vrabec, J.; Fischer, J. *Mol. Phys.*, in press.
(50) Smit, B.; Williams, C. P. *J. Phys.: Condes. Matter* **1990**, *2*, 4281.
(51) Pitzer, K. S. *J. Am. Chem. Soc.* **1955**, *77*, 3427.